DALTON
FULL PAPER

New ruthenium(II) and osmium(II) trinuclear dendrons. Synthesis, redox behavior, absorption spectra, and luminescence properties

Fausto Puntoriero,[a] Scolastica Serroni,*[a] Antonino Licciardello,[b] Margherita Venturi,[c] Alberto Juris,[c] Vittorio Ricevuto[a] and Sebastiano Campagna *[a]

[a] *Dipartimento di Chimica Inorganica, Chimica Analitica e Chimica Fisica, Università di Messina, Via Sperone 31, I-98166 Messina, Italy. Fax: Int.Code + (090) 393756; E-mail: photochem@chem.unime.it*
[b] *Dipartimento di Scienze Chimiche, Università di Catania, Viale A. Doria, I-95100 Catania, Italy*
[c] *Dipartimento di Chimica "G. Ciamician", Università di Bologna, Via F. Selmi 2, I-40126 Bologna, Italy*

Received 18th December 2000, Accepted 20th February 2001
First published as an Advance Article on the web 16th March 2001

The new trinuclear dendrons $[Cl_2Os\{(\mu\text{-}2,3\text{-}dpp)Ru(bpy)_2\}_2]^{4+}$ **3**, $\mathbf{Cl_2OsRu_2}$ (bpy = 2,2′-bipyridine; 2,3-dpp = 2,3-bis(2-pyridyl)pyrazine), $[Cl_2Os\{(\mu\text{-}2,3\text{-}dpp)Os(bpy)_2\}_2]^{4+}$ **4**, $\mathbf{Cl_2OsOs_2}$, and $[(bpy)Ru\{(\mu\text{-}2,3\text{-}dpp)Os(bpy)_2\}_2\}^{6+}$ **6**, $\mathbf{bpyRuOs_2}$ have been synthesized, and their redox properties, absorption spectra, and luminescence properties studied, together with the same properties of the species $[Cl_2Ru\{(\mu\text{-}2,3\text{-}dpp)Ru(bpy)_2\}_2]^{4+}$ **1**, $\mathbf{Cl_2RuRu_2}$, $[Cl_2Ru\{(\mu\text{-}2,3\text{-}dpp)Os(bpy)_2\}_2]^{4+}$ **2**, $\mathbf{Cl_2RuOs_2}$, and $[(bpy)Ru\{(\mu\text{-}2,3\text{-}dpp)Ru(bpy)_2\}_2\}^{6+}$ **5**, $\mathbf{bpyRuRu_2}$. All the compounds undergo several reversible metal-centered oxidation and ligand-centered reduction processes which are assigned to specific subunits of the trinuclear structure. Analysis of the reduction patterns of the various compounds allows one to obtain information on the extent of ligand–ligand interactions mediated by the central metals. The compounds show very intense ligand-centered absorption bands in the UV region and intense metal-to-ligand charge-transfer (MLCT) bands in the visible region, which can be assigned to transitions involving specific subunits of the dendron structure. All except **3** and **4** exhibit MLCT luminescence both at room temperature in acetonitrile fluid solution and in a MeOH–EtOH 4 : 1 (v/v) rigid matrix at 77 K. The luminescence properties are dominated by the photophysical properties of the subunit(s) in which the lowest-lying excited state of any structure is localized, suggesting that fast intercomponent energy transfer takes place in all the compounds.

Introduction

Luminescent and redox-active multinuclear metal complexes are playing a key role in the development of artificial systems exhibiting made-to-order properties. In particular, these species represent the basis for the design of molecular devices capable of using light energy to perform valuable functions, such as (i) conversion of solar energy into chemical energy[1] and (ii) elaboration of information at the molecular level.[2] As far as point (i) is concerned, dendrimers containing ruthenium(II) and/or osmium(II) polypyridine subunits are very interesting because of their ability, when properly designed, to behave as light-harvesting antenna systems.[3]

We have extensively been involved in the preparation and study of a series of ruthenium(II) and osmium(II) dendrimers in which 2,3-bis(2-pyridyl)pyrazine (2,3-dpp) acts as the bridging ligand to assembly the various metal subunits.[3–6] Many luminescent and redox-active dendrimers of this series have been synthesized and studied, with the larger systems containing as many as twentytwo metal subunits.[3,5] As for any type of dendrimer, the possibility to prepare large systems having the desired properties resides in the availability of specific building blocks.[7] Trinuclear species like $[Cl_2Ru\{(\mu\text{-}2,3\text{-}dpp)Ru(bpy)_2\}_2]^{4+}$ **1**, $\mathbf{Cl_2RuRu_2}$ (bpy = 2,2′-bipyridine)[4b] and $[Cl_2Ru\{(\mu\text{-}2,3\text{-}dpp)Os(bpy)_2\}_2]^{4+}$ **2**, $\mathbf{Cl_2RuOs_2}$[4c] have indeed been essential to build up most of the larger species of the series, through convergent or semi-convergent routes, by taking advantage of the labile chloride ligands of the central metal.[6,8] So, **1** and **2** may be considered "active" dendrons, in the sense that they can be employed in the construction of larger dendrimers.

Here we report the synthesis of new trinuclear dendrons of this series, namely $[Cl_2Os\{(\mu\text{-}2,3\text{-}dpp)Ru(bpy)_2\}_2]^{4+}$ **3**, $\mathbf{Cl_2OsRu_2}$ and $[Cl_2Os\{(\mu\text{-}2,3\text{-}dpp)Os(bpy)_2\}_2]^{4+}$ **4**, $\mathbf{Cl_2OsOs_2}$, and a detailed study of the redox behavior, absorption spectra and photophysical properties of the complete series of active trinuclear dendrons **1**–**4**, as well as of the trinuclear species $[(bpy)Ru\{(\mu\text{-}2,3\text{-}dpp)Ru(bpy)_2\}_2\}^{6+}$ **5**, $\mathbf{bpyRuRu_2}$ and $[(bpy)Ru\{(\mu\text{-}2,3\text{-}dpp)Os(bpy)_2\}_2]^{6+}$ **6**, $\mathbf{bpyRuOs_2}$. Absorption and photophysical properties of **5** have been reported,[4a] but they have been re-examined and discussed here for comparison purposes. Compounds **5** and **6** are "synthetically inactive" species, in the sense that they cannot be used for dendrimer synthesis because they do not contain labile ligands, but their properties are of importance since they can mimic the properties of the trinuclear dendrons inserted in larger structures. It should be also pointed out that the trinuclear dendrons **3** and **4** open the way to obtain high generation dendrimers containing osmium centers at intermediate sites, not available up to now. The structural formulas of all the species investigated here are shown in Fig. 1.

The results obtained by this investigation allowed us to gain knowledge on the electronic interactions among the various components of the multicomponent-structured trinuclear dendrons, and will be very useful for designing larger species with predetermined redox and photophysical properties.

Experimental

General information

2,3-Bis(2-pyridyl)pyrazine (2,3-dpp),[9] $Ru(bpy)_2Cl_2$,[10a] $Os(bpy)_2Cl_2$,[10b] $[Ru(bpy)_2(2,3\text{-dpp})]^{2+}$,[4a] and $[Os(bpy)_2(2,3\text{-dpp})]^{2+}$[11] were prepared following literature procedures. $RuCl_3\cdot 3H_2O$ and K_2OsCl_6 were purchased by Aldrich. All reactions were carried out under argon.

Syntheses

$[Cl_2Ru\{(\mu\text{-}2,3\text{-dpp})Ru(bpy)_2\}_2][PF_6]_4$ 1, Cl_2RuRu_2. A mixture of $[Ru(bpy)_2(2,3\text{-dpp})][PF_6]_2$ (80 mg, 0.085 mmol), $RuCl_3\cdot 3H_2O$ (11.5 mg, 0.042 mmol) and LiCl (12 mg, 0.028 mmol) in ethanol (15 mL) was refluxed for 26 h. After cooling to room temperature, an excess of solid NH_4PF_6 was added. A dark green precipitate was formed, which was isolated by filtration and washed several times with ethanol. The purification was achieved by column chomatography on neutral aluminium oxide (diameter 2.5 cm; length 20 cm; aluminium oxide activity 1), eluting with CH_3CN–toluene 1 : 1 (v/v). The first band eluted (orange) contained unchanged mononuclear complex. The amount of CH_3CN in the eluent was then increased progressively (up to 3 : 1 (v/v) CH_3CN–toluene) in order to obtain the green-blue product, which was rotary evaporated to dryness. The product was then dissolved in 2 mL of CH_3CN and precipitated by addition of diethyl ether. The yield after purification was 55%. TOF-SIMS (time-of-flight secondary ion mass spectrometry): $[M - PF_6]^+$, calc. *m*/*z* 1902.3228, found 1902.3218. Elemental analysis: calculated (found) for $C_{68}H_{52}Cl_2F_{24}N_{16}P_4Ru_3$ (%) C, 39.90 (39.82); H, 2.56 (2.48); N, 10.95 (10.90).

$[Cl_2Ru\{(\mu\text{-}2,3\text{-dpp})Os(bpy)_2\}_2][PF_6]_4$ 2, Cl_2RuOs_2. A mixture of $[Os(bpy)_2(2,3\text{-dpp})][PF_6]_2$ (85 mg, 0.083 mmol), $RuCl_3\cdot 3H_2O$ (10.8 mg, 0.041 mmol) in ethylene glycol–MeOH 3 : 1 (v/v) (8 mL) was refluxed for 28 h. To the cooled mixture, 6 mL of a saturated aqueous solution of NH_4PF_6 were added. The blue solid precipitate was washed several times with cold ethanol. Chromatographic and subsequent treatment procedures were similar to those for compound **1**. The yield was 57%. TOF-SIMS: $[M - PF_6]^+$, calc. *m*/*z* 2080.5946, found 2080.5940. Elemental analysis: calculated (found) for $C_{68}H_{52}Cl_2F_{24}N_{16}Os_2P_4Ru$ (%): C, 36.70 (36.80); H, 2.36 (2.29); N, 10.07 (10.20).

$[Cl_2Os\{(\mu\text{-}2,3\text{-dpp})Ru(bpy)_2\}_2][PF_6]_4$ 3, Cl_2OsRu_2. $[Ru(bpy)_2(2,3\text{-dpp})][PF_6]_2$ (153 mg, 0.163 mmol) and K_2OsCl_6 (39 mg, 0.0815 mmol) were allowed to react in refluxing ethylene glycol (4 mL) for 7 h, and the cooled mixture treated with 5 mL of a saturated aqueous solution of sodium dithionite. After addition of an excess of solid NH_4PF_6 a dark blue precipitate was formed, which was isolated by filtration and washed several times with water, then purified as described for complex **1**. The yield was 67%. TOF-SIMS: $[M - PF_6]^+$, calc. *m*/*z* 1991.4346, found 1991.4334. Elemental analysis: calculated (found) for $C_{68}H_{52}Cl_2F_{24}N_{16}OsP_4Ru_2$ (%): C, 38.23 (38.32); H, 2.45 (2.51); N, 10.49 (10.30).

$[Cl_2Os\{(\mu\text{-}2,3\text{-dpp})Os(bpy)_2\}_2][PF_6]_4$ 4, Cl_2OsOs_2. To a stirred solution of K_2OsCl_6 (14 mg, 0.029 mmol) in ethylene glycol (4 mL) was added $[Os(bpy)_2(2,3\text{-dpp})][PF_6]_2$ (60 mg, 0.058 mmol). The mixture was refluxed for 2 h, cooled at room temperature and then treated with 5 mL of a saturated aqueous solution of sodium dithionite. An excess of solid NH_4PF_6 was added, the dark precipitate formed was isolated by filtration and washed several times with water, then purified as described for complex **1**. The yield was 68%. TOF-SIMS: $[M - PF_6]^+$, calc. *m*/*z* 2169.5998, found 2169.5992. Elemental analysis: calculated (found) for $C_{68}H_{52}Cl_2F_{24}N_{16}Os_3P_4$ (%): C, 35.29 (35.28); H, 2.26 (2.32); N, 9.68 (9.79).

$[(bpy)Ru\{(\mu\text{-}2,3\text{-dpp})Ru(bpy)_2\}_2][PF_6]_6$ 5, $bpyRuRu_2$. A mixture of complex **1** (40 mg, 0.0195 mmol), bpy (3.1 mg, 0.0195 mmol) and $AgNO_3$ (6.6 mg, 0.039 mmol) in 6 mL of ethanol–water 1 : 1 (v/v) was refluxed for 60 h. The cooled solution was centrifuged to remove AgCl. After addition of an excess of solid NH_4PF_6 the violet precipitate formed was isolated by filtration and purified by column chromatography on neutral aluminium oxide (diameter 2.5 cm; length 20 cm; aluminium oxide activity 1), eluting with 9 : 1 (v/v) CH_2Cl_2–MeOH. The second band obtained (violet) was rotary evaporated and the residue dissolved in a small amount of CH_3CN and precipitated by addition of diethyl ether. The final product was a violet solid (58%). TOF-SIMS: $[M - PF_6]^+$, calc. *m*/*z* 2277.4838, found 2277.4828. Elemental analysis: calculated (found) for $C_{78}H_{60}F_{32}N_{18}P_6Ru_3$ (%): C, 38.67 (38.72); H, 2.50 (2.48); N, 10.41 (10.30).

$[(bpy)Ru\{(\mu\text{-}2,3\text{-dpp})Os(bpy)_2\}_2][PF_6]_6$ 6, $bpyRuOs_2$. Complex **2** (40 mg, 0.018 mmol), bpy (2.8 mg, 0.018 mmol) and $AgNO_3$ (6.4 mg, 0.0347 mmol) were refluxed in 6 mL of ethanol–water 1 : 1 (v/v) for 120 h. The cooled mixture was centrifuged to remove AgCl. When an excess of solid NH_4PF_6 was added a violet precipitate was obtained and isolated by filtration. Chromatographic and subsequent treatment procedures were similar to those for **5**. The yield was 50%. TOF-SIMS: $[M - PF_6]^+$, calc. *m*/*z* 2455.7438, found 2455.7430. Elemental analysis: calculated (found) for $C_{78}H_{60}F_{32}N_{18}Os_2P_6Ru$ (%): C, 36.02 (36.12); H, 2.33 (2.25); N, 9.69 (9.52).

Equipment and procedures

Electrochemical measurements were carried out in argon-purged acetonitrile at room temperature with PAR 273 multipurpose equipment interfaced to a PC. The working electrode was a glassy carbon (8 mm^2, Amel) electrode. The counter electrode was a platinum wire, and the reference electrode was an SCE separated with a fine glass frit. The concentration of the complexes was about 5×10^{-4} M. Tetrabutylammonium hexafluorophosphate was used as supporting electrolyte and its concentration was 0.05 M. Cyclic voltammograms were obtained at scan rates of 20, 50, 200, and 500 mV s^{-1}. For reversible processes, half-wave potentials (*vs.* SCE) were calculated as the average of the cathodic and anodic peaks. The criteria for reversibility were the separation of 60 mV between cathodic and anodic peaks, the close to unity ratio of the intensities of the cathodic and anodic currents, and the constancy of the peak potential on changing scan rate. The number of exchanged electrons was measured with differential pulse voltammetry (DPV) experiments performed with a scan rate of 20 mV s^{-1}, a pulse height of 75 mV, and a duration of 40 ms, and by taking advantage of the presence of ferrocene used as the internal reference. Mass spectra were obtained by TOF-SIMS experiments. Experimental details on this method applied to metal dendrimers and dendrons will be reported elsewhere.[12] Absorption spectra were recorded with a Kontron Uvikon 860 spectrophotometer, luminescence spectra up to 900 nm with a Spex-Jobin Yvon Fluoromax-2 spectrofluorimeter equipped with a Hamamatsu R3896 photomultiplier, corrected for photomultiplier response using a program purchased with the fluorimeter. For luminescence spectra at wavelengths longer than 900 nm the 514 nm line of a Spectra-Physics 265 argon laser was used for excitation in a modified Edinburgh FS900 spectrofluorimeter. Detection was accomplished using a cooled (77 K) North Coast EO-817L germanium detector in combination with a Stanford Research SR lock-in amplifier. Emission lifetimes were measured with an Edinburgh FL-900 single-photon counting spectrometer (nitrogen discharge; pulse width, 3 ns). Emission quantum yields were measured at room temperature (20 °C) using the optically dilute method.[13] $[Ru(bpy)_3]^{2+}$ in aerated aqueous solution was used as a

quantum yield standard, assuming a value of 0.028.[14] For emitters with λ_{max} longer than 850 nm, emission lifetimes and quantum yields were not obtained because of technical problems. Experimental uncertainties were as follows: absorption maxima, ±2 nm; molar absorption coefficient, 10%; emission maxima, ±5 nm in the visible region and ±10 nm in the near-IR region; excited state lifetimes, 10%; luminescence quantum yields, 20%; redox potentials, ±10 mV.

Results

All the compounds studied are stable in acetonitrile solution for weeks, as demonstrated by the constancy of their absorption spectra. Their cyclic voltammograms show a reversible oxidation process and at least two reversible reduction processes in the potential window examined (+2.00/−1.20 V *vs.* SCE). The cyclic voltammograms of the series $Cl_2MM'_2$ **1**–**4** also show a second reversible oxidation process, which is absent in those of **5** and **6**. However, differential pulse voltammetry showed that all the complexes undergo two oxidation process, with the one occurring at more positive potentials for **5** and **6** peaking at the limit of the potential window examined. This circumstance most likely made it difficult to observe the second oxidation process of **5** and **6** in the cyclic voltammetry experiments. From comparison of the areas of the peaks, the first oxidation process of **1**–**4** is monoelectronic in nature and the second one is bielectronic, whereas the opposite occurs for **5** and **6**. The cyclic and differential pulse voltammetries of **5** and **6** also reveal two additional reduction processes in the potential window examined, which are not seen for **1**–**4**. All the reduction processes are monoelectronic.

The absorption spectra of all the compounds are dominated by intense bands which extend throughout the UV-visible region. In particular, very intense bands are present in the UV region (ε in the 10^5–10^6 M^{-1} cm^{-1} range) and moderately intense bands are present in the visible region (ε in the 10^4–10^5 M^{-1} cm^{-1} range).

All the compounds studied except **3** and **4** exhibit luminescence, both at room temperature in fluid solution and at 77 K in a rigid matrix. The emission spectra are in all the cases medium-dependent, moving to higher energy on passing from room to glass temperature. Luminescence lifetimes and quantum yields have been measured only for **5**, because for the other complexes emission occurs in the near-infrared region, and our equipment is unable to measure luminescence lifetimes and quantum yields in that region.

Table 1 collects the redox data of all the multinuclear compounds. Figs. 2–4 show the oxidative differential pulse voltammograms of **1**–**6**, Fig. 5 shows the cyclic voltammogram of **5**. Figs. 6 and 7 show the absorption spectra of **3**–**6**, and Fig. 8 shows the luminescence spectra (at room temperature) of **1**, **2**, and **6**. The relevant absorption and luminescence data are gathered in Table 2.

Discussion

The spectroscopic and photophysical properties and redox behavior of transition metal complexes are usually discussed with the assumption that the ground state, as well as the excited and redox states, can be described by a localized molecular orbital configuration.[15–18] Within this framework the various spectroscopic transitions and excited states are classified as metal-centered (MC), ligand-centered (LC), or charge-transfer (either metal-to-ligand, MLCT, or ligand-to-metal, LMCT), and the oxidation and reduction processes are classified as metal- or ligand-centered.[15–18]

In metal-based multicomponent systems like the ones reported in this paper the electronic interactions between the metal components, mediated by the bridging ligands, are relatively weak, so that the redox processes, as well as the luminescence and absorption features, may be attributed to specific subunits of the array.[1b,5,6] This approach has proved to be quite powerful, so that we will use it in the following discussion.

Table 1 Electrochemical data[a]

Compound	$E_{1/2}$(ox)/V *vs.* SCE	$E_{1/2}$(red)/V *vs.* SCE	ΔE[b]
1 Cl_2RuRu_2	+0.82 [1]; +1.57 [2]	−0.72 [1]; −0.88 [1]	0.16
2 Cl_2RuOs_2	+0.74 [1]; +1.16 [2]	−0.72 [1]; −0.87 [1]	0.15
3 Cl_2OsRu_2	+0.57 [1]; +1.55 [2]	−0.71 [1]; −0.96 [1]	0.25
4 Cl_2OsOs_2	+0.51 [1]; +1.16 [2]	−0.69 [1]; −0.91 [1]	0.22
5 $bpyRuRu_2$	+1.51 [2]; +1.95 [1]	−0.52 [1]; −0.66 [1] −1.13 [1]; −1.23 [1]	0.14
6 $bpyRuOs_2$	+1.11 [2]; +1.94 [1]	−0.52 [1]; −0.65 [1] −1.08 [1]; −1.16 [1]	0.13

[a] Acetonitrile solution, room temperature. The number of exchanged electrons is reported in square brackets; experimental error, ±10 mV. [b] Difference (in V) between first and second reduction process.

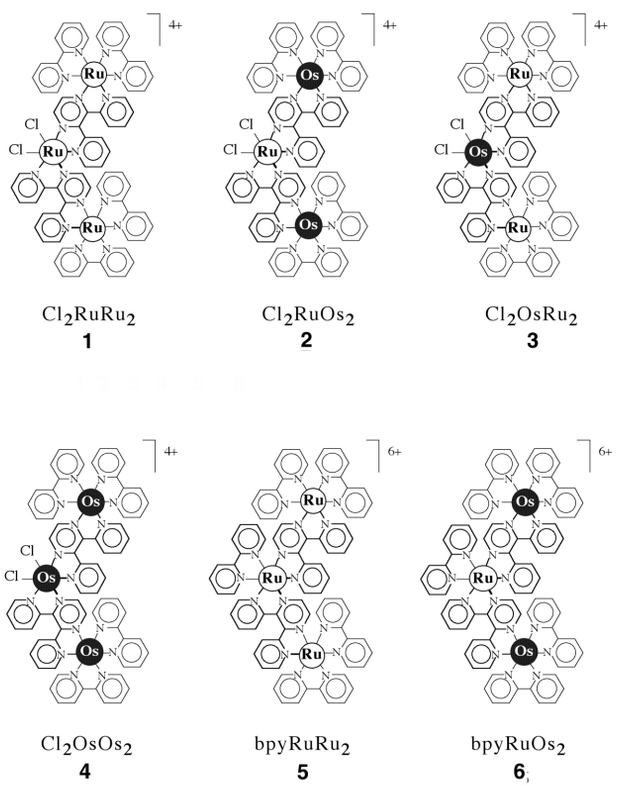

Fig. 1 Structural formulas and acronyms of the compounds.

Redox behavior

Oxidation. As observed for the metal-based dendrimers of this series, the reversible oxidation processes exhibited by the trinuclear compounds studied here can be assigned to metal-centered processes.[19] For the assignment of the various processes to specific subunits of the arrays we will start the discussion with **4**. This species contains three osmium(II) subunits (see Fig. 1): however, the central osmium is quite different from the peripheral subunits because of the different chemical environment. In particular, it has a higher electron density than the peripheral ones, as a consequence of the electron donating ability of the two chloride ligands, and therefore should be oxidized at a less positive potential. The experimental results (Table 1, Fig. 3) are consistent with such a hypothesis: the process at less positive potential is indeed monoelectronic and may be assigned to the central metal oxidation. The potential for oxidation of the central osmium is also consistent with that of $Os(biq)_2Cl_2$ (biq = 2,2′-biquinoline), which is +0.25 V *vs.* SCE

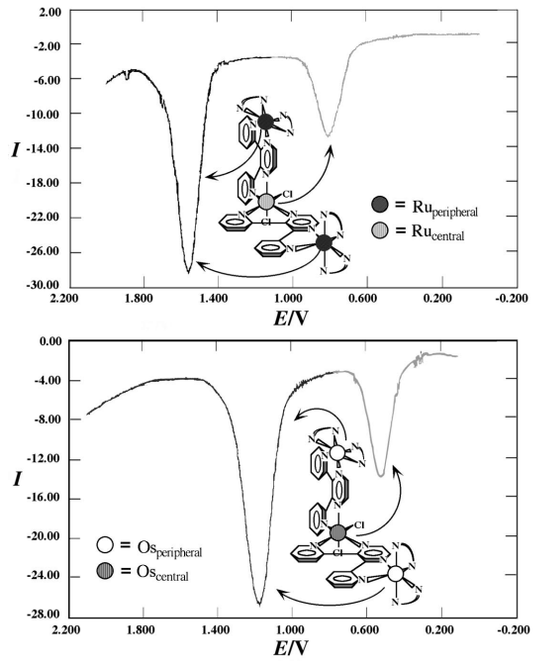

Fig. 2 Differential pulse voltammograms of complexes **1** (top) and **4** (bottom) in acetonitrile. In the compound structure NN stands for bpy.

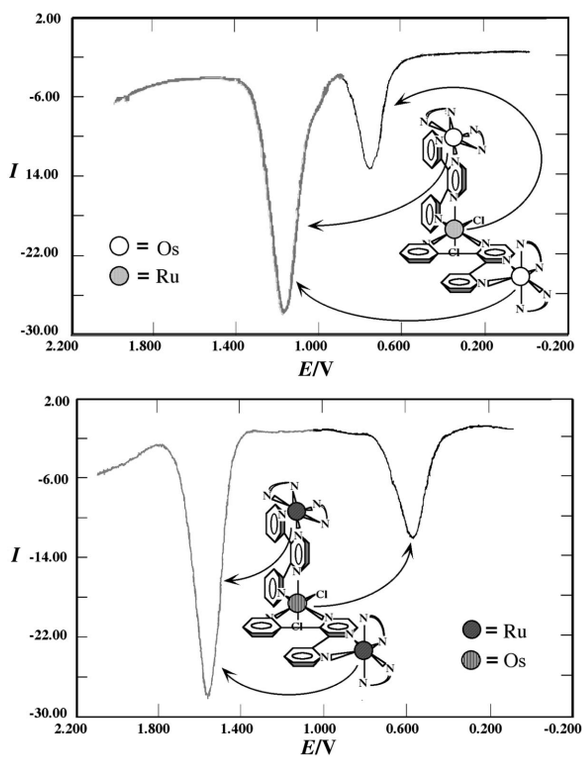

Fig. 3 Differential pulse voltammograms of complexes **2** (top) and **3** (bottom) in acetonitrile.

in acetonitrile solution:[11] in the modular approach to multicomponent species, the peripheral $\{(\mu\text{-}2,3\text{-dpp})Os(bpy)_2\}^{2+}$ subunits may be seen as "ligands" of the central osmium. These latter positively charged ligands are better electron withdrawing groups than the neutral biq ligands, so that they make oxidation of the osmium center more difficult in **4** than in $Os(biq)_2Cl_2$. The second oxidation process of **4** is bielectronic and can be safely assigned to simultaneous one-electron oxidation of the two non-interacting peripheral osmium ions.

On the basis of the above discussion, the assignment of the oxidation processes of complex **1** (Table 1, Fig. 2) is straightforward: the first, monoelectronic process involves oxidation of the central ruthenium ion, and the second, bielectronic process is assigned to simultaneous one-electron oxidation of the two non-interacting peripheral ruthenium centers. The difference in the potentials between **1** and **4** is due to the different oxidizability of Ru^{II} and Os^{II}.

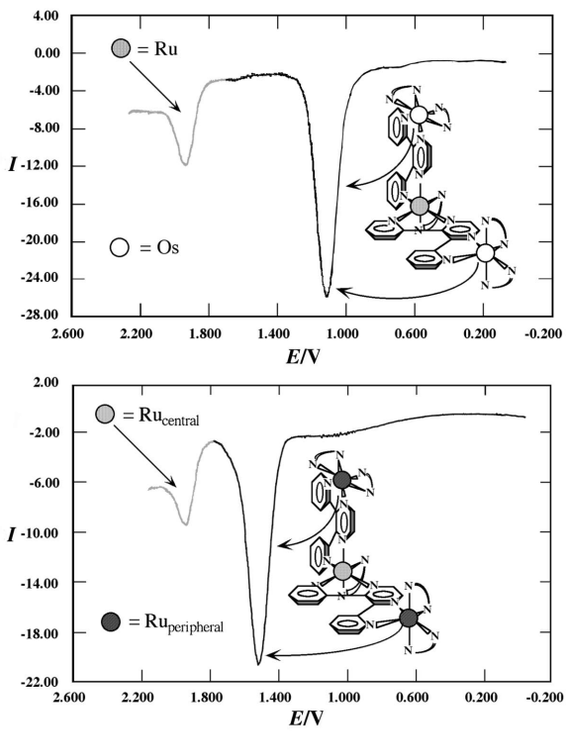

Fig. 4 Differential pulse voltammograms of complexes **6** (top) and **5** (bottom) in acetonitrile.

The assignment of the oxidation processes of complexes **2** and **3** (Table 1, Figs. 2 and 3) is simplified by comparison of the oxidation data of these compounds (*i.e.* the potentials and the number of exchanged electrons) with those of **1** and **4**. This analysis allows us safely to assign the first, monoelectronic, oxidation process of **3** to the central osmium ion and the successive, bielectronic process to simultaneous oxidation of the two peripheral Ru-based subunits. The opposite assignment (*i.e.* the first process to the central Ru and the second, bielectronic process to the peripheral osmium centers) holds for **2**.

Comparisons among the potentials for oxidation processes of the various subunits in the series of the trinuclear $Cl_2MM'_2$ dendrons (Table 1) evidence some intriguing features. For example, the value of the oxidation of the $\{Cl_2Os(\mu\text{-}2,3\text{-dpp})_2\}$ subunit (*i.e.* the central osmium subunit) in complex **4** is slightly less positive (60 mV) than that of the same subunit in the mixed-metal species **3**. This can be rationalized by taking into account that the peripheral subunits which are present in **4**, *i.e.* $\{(\mu\text{-}2,3\text{-dpp})Os(bpy)_2\}^{2+}$, have a better electron donating ability than those in **3**, *i.e.* $\{(\mu\text{-}2,3\text{-dpp})Ru(bpy)_2\}^{2+}$, because back donation (or π donation) from osmium(II) to the bridging ligand is more effective than from ruthenium(II). The same argument explains why the potential of the oxidation of the $\{Cl_2Ru(\mu\text{-}2,3\text{-dpp})_2\}$ subunit (*i.e.* the central ruthenium subunit) in **2** is more positive (80 mV) than the that of the same unit in **1**.

As far as species **5** and **6** are concerned, the presence of a bpy ligand instead of two chlorides in the coordination sphere of the central ruthenium significantly modifies the redox properties of this site. Also in this case, assignment of the processes to specific building blocks is allowed by comparison of potentials and numbers of exchanged electrons of the various compounds given in Table 1. In **5** (Table 1, Fig. 4) the first oxidation

process is bielectronic, and occurs at a potential close to that obtained for oxidation of the peripheral sites of **1** and **3**. As a consequence, this process is assigned to the simultaneous, one-electron oxidation of the two peripheral, Ru-based components. The monoelectronic oxidation occurring close to the upper limit of the accessible potential window is assigned to oxidation of the central $\{(bpy)Ru(\mu\text{-}2,3\text{-}dpp)_2\}^{2+}$ subunit. It is also interesting to compare this potential to that of subunits of the type $\{Ru(\mu\text{-}2,3\text{-}dpp)_3\}^{2+}$, which are present as intermediate chromophoric and redox-active sites in deca- and hexa-nuclear dendrimers of this family. These latter subunits are oxidized at around +2.1 V (in liquid SO_2 at −70 °C),[4i] that is a more positive potential with respect to that found here for the $\{(bpy)Ru(\mu\text{-}2,3\text{-}dpp)_2\}^{2+}$ subunit, consistent with the different electron withdrawing abilities of bpy and μ-2,3-dpp ligands.[5b]

For complex **6** (Table 1, Fig. 4) an analogous interpretation is proposed for the observed oxidation pattern. The first process, bielectronic, involves the two peripheral Os-based subunits, and the second one, monoelectronic, is assigned to the central, Ru-based, component. In spite of the different peripheral metals and differently from what is found for the $Cl_2MM'_2$ series of compounds, there is no significant difference between the central metal oxidation potential in the $bpyRuM'_2$ series of complexes, thus indicating that the electron donating abilities of the peripheral groups $\{(\mu\text{-}2,3\text{-}dpp)Ru(bpy)_2\}^{3+}$ and $\{(\mu\text{-}2,3\text{-}dpp)Os(bpy)_2\}^{3+}$ are quite close one another once the metals are oxidized.

It can be noted that the peripheral subunit oxidation in compounds of the $bpyRuM'_2$ series occurs at a potential slightly less positive than that of the corresponding oxidation in analogous compounds of the $Cl_2MM'_2$ series. It should be considered, however, that such oxidation processes in the latter compounds take place in the presence of an already oxidized central metal.

An interesting feature appears on looking at Fig. 9, in which the potential values for the oxidation of the various species are reported together with the relative assignments. It shows that the oxidation of a specific subunit of the multicomponent systems studied here, even on taking into account slight modifications induced by the other subunits present in the multicomponent structures and discussed above, always takes place within a relatively confined potential window. This strongly indicates that, to a first approximation, each individual subunit maintains its own redox properties in the supramolecular arrangements.

Reduction. The reversible, reduction processes of the compounds may be assigned to the polypyridine ligands, in agreement with the redox behavior of similar compounds.[4–6,19] It is indeed known by former studies that in multinuclear metal complexes each 2,3-dpp bridging ligand is reversibly reduced twice at potentials less negative than −1.2 V before bpy reduction takes place, usually at potentials more negative than −1.5 V.[4a,5b] As a consequence, the first two reductions of the complexes (Table 1, Fig. 5) are assigned to the first reduction of each dpp ligand and, as far as **5** and **6** are concerned, the third and fourth reductions, only visible for these latter species, to the second reduction processes centered again in the same ligand. This assignment is also consistent with the difference between second and third reduction potentials, which is around 400 mV, a typical pairing energy for the two added electrons in the dpp ligand.[4a,5b] Also on the basis of the above discussion, we believe that the second reduction of each bridging ligand in **1**–**4** is displayed out of the examined potential window.

A general consideration which can be made on looking at the data gathered in Table 1 is that the reduction potentials for compounds of the $bpyRuM_2$ series are less negative than those of corresponding species of the $Cl_2MM'_2$ series. This is rationalizable on considering the different electron donating abilities of bpy and chloride ligands.

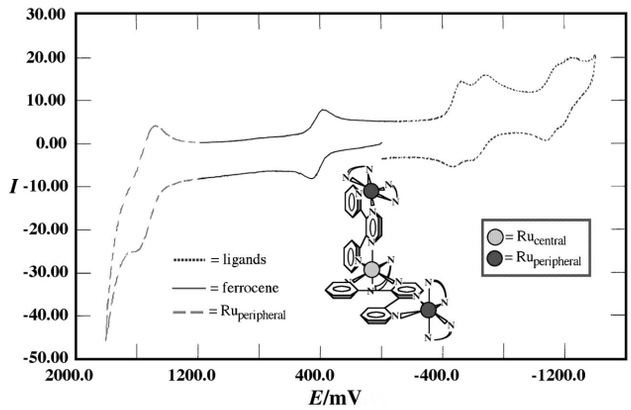

Fig. 5 Cyclic voltammetry curve of complex **5**. The full line shows the process due to ferrocene, used as reference.

It is instructive to compare the separation between the first and second reductions of compounds **1**–**4**. Such reductions are centered on the two bridging ligands and their separation is related to the interaction between the ligands, in its turn connected to electrostatic (coulombic) and electronic factors. In **1**–**4** the Coulombic factor is constant, at a first approximation, so that the difference in the separation between the two reduction processes for these compounds is a direct consequence of the electronic interaction between the bridging ligands, as mediated by the central metal. Such an interaction involves the (ligand-centered) π_L^* orbitals, where the added electrons are localized, and is mediated by the (metal-centered) π_M orbitals. A determinant factor for the interaction is the energy difference between the π_L^* orbitals and the π_M orbitals.[20] The energy difference is smaller when the metal involved is osmium, because the full π_{Os} orbitals lie at higher energy (and therefore closer to the empty π_L^* orbitals) than π_{Ru} orbitals in analogous compounds. On the basis of the above discussion, it is clear why the ligand–ligand interaction, as inferred by the reduction potentials (Table 1), is larger in **4** and **3**, in which the reduction sites are linked to an osmium center, than in **1** and **2**, in which the interaction is mediated by a ruthenium center.

The same arguments also allow one to explain why the ligand–ligand interaction between the monoreduced bridging ligands (inferred by the separation between the third and fourth reduction processes) is reduced when compared to that in the ground state (inferred by the separation between the first couple of reduction processes), as evidenced by complexes **5** and **6**. In fact, the separation between the first and second reductions of the two complexes, 0.14 and 0.13 V, respectively, decreases to 0.10 and 0.08 V, respectively, on passing to the third and fourth reduction processes (see Fig. 5). This can be attributed to the increase of the energy level of the π* ligand orbitals upon addition of the first two electrons (one for each bridging ligand), which translates into a larger energy difference between ligand-centered π_L^* and metal-centered π_M orbitals.

Absorption spectra

On the basis of the molar absorption coefficients (Table 2, Figs. 6 and 7) and literature data,[4–6,16] for all the complexes the absorption bands in the UV region may be assigned to spin-allowed LC transitions, those in the visible to spin-allowed and/or spin-forbidden MLCT transitions. In particular, the absorption bands which exhibit a maximum at about 285 nm (Table 2, Figs. 6 and 7) receive a main contribution from bpy-centered transitions, while the feature present in the 300–360 nm region is mainly attributed to dpp-centered transitions.

The assignment of the broad bands in the visible region to specific transitions and sites is more complicated because of the presence of many possible MLCT transitions. The different types of MLCT transitions which may occur in the trinuclear

Table 2 Spectroscopic and photophysical data

Compound	Absorption[a] λ_{max}/nm (ε/M^{-1} cm^{-1})	Luminescence, λ_{max}/nm	
		298 K[a]	77 K[b]
1 Cl_2RuRu_2	283 (111300) 434 (21100) 494 (19700) 625 (26100)	904	860
2 Cl_2RuOs_2	286 (160200) 432 (30300) 586 (39100)	952	885
3 Cl_2OsRu_2	284 (113500) 436 (22300) 620 (24900)	[c]	[c]
4 Cl_2OsOs_2	287 (114600) 445 (24300) 591 (26000)	[c]	[c]
5 bpyRuRu$_2$[d]	282 (193400) 425 (35700) 545 (23500)	802[e]	710[f]
6 bpyRuOs$_2$	286 (156200) 425 (22200) 559 (31900)	965	890

[a] Acetonitrile deoxygenated solution. [b] MeOH–EtOH (4 : 1) rigid matrix. [c] No emission detectable for $\lambda < 1800$ nm. [d] Data from ref. 4(*a*). [e] $\tau = 125$ ns, $\varphi = 0.003$. [f] $\tau = 2.0$ μs.

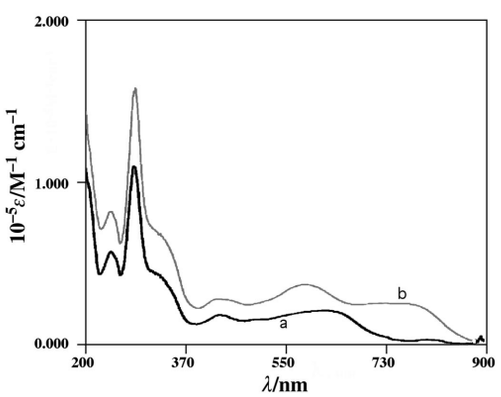

Fig. 6 Absorption spectra of complexes **3** (a) and **4** (b) in acetonitrile.

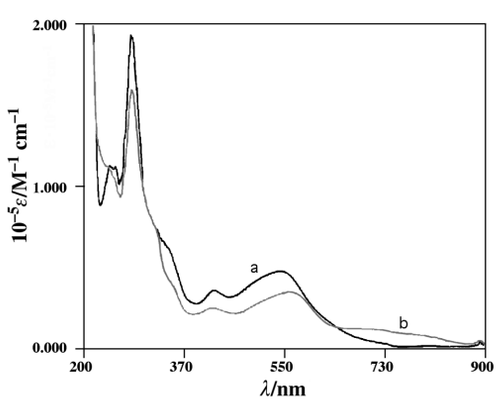

Fig. 7 Absorption spectra of complexes **5** (a) and **6** (b) in acetonitrile.

compounds studied here are shown in Fig. 10.[24] The redox data (Table 1) are very useful to determine the energy order of such MLCT transitions in the various complexes. In the homometallic trinuclear dendrons **1** and **4** the order of the transitions schematized in Fig. 10 is e < f < g. The bands peaking at 625, 494, and 434 nm in the absorption spectrum of **1** and those peaking (or exhibiting a shoulder) at 591, 540, and 445 nm in the spectrum of **4** (Table 2, Fig. 6) may therefore be assigned to e-, f-, and g-type spin-allowed MLCT transitions, respectively. For **4**, the absorption bands at wavelengths longer than 730 nm can be assigned to spin-forbidden MLCT transitions, which steal intensity from the spin-allowed bands because of the strong spin–orbit coupling induced by the heavier metal center.

The same energy order of the e, f, and g MLCT transitions also holds for complexes **2** and **3**, so the assignment of their visible bands is straightforward, including the less intense transitions at $\lambda > 730$ nm (Fig. 6), which are due to spin-forbidden transitions involving the osmium centers.

For complex **5** the energy order of the MLCT transitions, with reference to Fig. 10, should be a < b < c < d. In fact, the band at 625 nm, which is present for **1** and attributed to the e-type MLCT transition, is absent for **5**, where the e-type transition has no counterpart (it is in fact absent for the "Cl_2Ru" donor group). The transitions b and a (and, to a minor extent, c) of the bpyRuM$_2$ complexes have counterparts in the e and f (and g) transitions in the $Cl_2MM'_2$ series. However, b and a transitions are different in energy from their analogous ones of the $ClMM'_2$ series, because of the differences in the energies of polypyridine- and metal-centered orbitals in the two series of compounds. On the basis of the above discussion, the band peaking at 545 nm can be mainly assigned to the a transition and that peaking at 425 nm to transitions c and d. Transition b contributes to the blue side of the main visible band. This assignment agrees with that reported for this species.[4a]

For complex **6** the assignment of the visible spectrum to specific transitions is very similar to that of **5**, with the exception of the large band at $\lambda > 610$ nm, which is due to spin-forbidden MLCT transitions involving the osmium centers.

Luminescence properties

In multicomponent species like the ones studied here the lowest-energy excited state of each individual subunit, populated within the subpicosecond timescale with unitary efficiency from upper-lying levels centered in that subunit,[25] may directly decay to the ground state or may transfer its electronic energy to suitable nearby subunits by energy transfer (electron transfer processes are disregarded in the present discussion, as well as other types of excited state interactions, because energy transfer is the sole intercomponent deactivation process which may play a significant role in the studied complexes on thermodynamic bases) if sufficient electronic coupling between the subunits exists.[1] Therefore, the fate of any subunit-localized excited state in the multicomponent structure depends on the electronic coupling between the subunits of the arrays and on the presence of lower-lying excited states in nearby subunits.

All the building blocks which are present in the systems studied here are expected to be luminescent from ^{3}MLCT excited states,[3–6,26,27] so in principle multiple emission could take place in each dendron. However, the 2,3-dpp bridging ligand has been reported to allow very fast energy transfer processes between the metal-based subunits it connects,[3–6] and single luminescence, involving the subunit(s) where the lowest-lying excited state of the whole species is located, should take place.

The lowest-lying, intrinsically luminescent ^{3}MLCT level of the peripheral subunit $\{(\mu\text{-}2,3\text{-}dpp)Ru(bpy)_2\}^{2+}$, which is present in complexes **1**, **3**, and **5**, is known to exhibit luminescence at about 800 nm in fluid solution at room temperature and at about 720 nm in a rigid matrix at 77 K.[3–6] This is confirmed in **5** (Table 2) where the central Ru-based chromophore is expected to lie at higher energy.[3–6] However in **1** and **3** the lowest-lying ^{3}MLCT states of the central subunits ($\{Cl_2Ru(\mu\text{-}2,3\text{-}dpp)_2\}$ and $\{Cl_2Os(\mu\text{-}2,3\text{-}dpp)_2\}^{2+}$, respectively) should lie at lower energies, on the basis of the redox data. Indeed, the luminescence spectra of **1** both at room temperature and at 77 K (Table 2, Fig. 8) are significantly red-shifted compared to those of **5**, and can safely be assigned to the triplet MLCT levels involving the central metal. The lowest-lying MLCT state of compound **3** is expected to lie below 1000 nm, anyway **3** does not exhibit

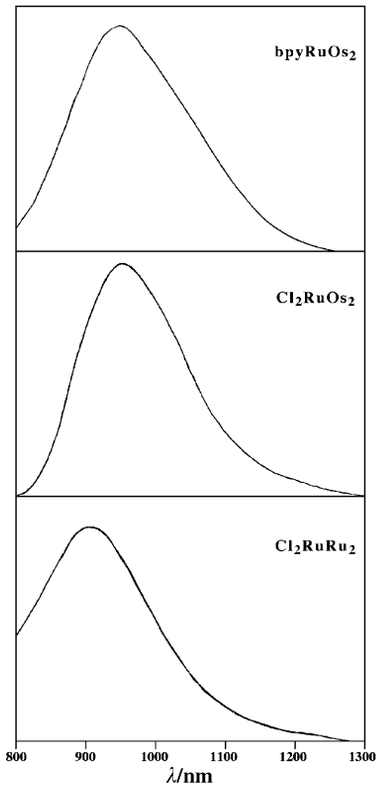

Fig. 8 Luminescence spectra of complexes **1**, **2**, and **6** in acetonitrile at room temperature.

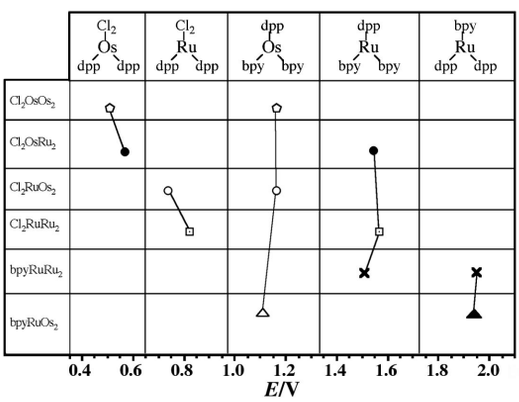

Fig. 9 Schematic representation of the potentials for oxidation of complexes **1**–**6** as a function of the redox-active subunits.

any luminescence, either at room temperature or at 77 K. Most likely due to the energy gap law the rate constants of the radiationless transitions for the lowest-lying MLCT state of **3** are so large that the luminescence becomes undetectable with our equipment. The same arguments can also justify the absence of luminescence of **4**, where the same lowest-lying MLCT level of **3** is present.

The luminescence properties of complex **6** both at room temperature and 77 K (Table 2, Fig. 8) are very similar to those of the other species containing the $\{(\mu\text{-}2,3\text{-dpp})Os(bpy)_2\}^{2+}$ subunit(s), so they may be straightforwardly attributed to the ^{3}MLCT levels involving this subunit.

The attribution of the luminescence spectra of complex **2** to a specific subunit is not that straightforward. On the basis of the redox data and of the usual correlation between spectroscopic and electrochemical data commonly found for metal polypyridine MLCT emitters,[28] the MLCT state involving the central, Ru-based subunit was expected at lower energy than the MLCT state involving the peripheral, Os-based subunits. However, a comparison between the luminescence spectra of **1**

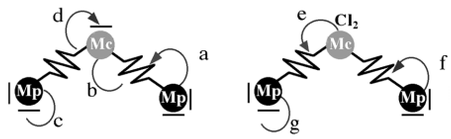

Fig. 10 Schematization of the trinuclear dendrons and of the expected MLCT transitions involving peripheral (Mp) and central (Mc) metals (for details, see text).

and **6** indicates that this is not the case and demonstrates that the spectroscopy/electrochemistry correlation does not hold for the individual subunits studied here. This is not a totally surprising result, since the stabilization of redox and excited states may be significantly different in ruthenium and osmium subunits and in subunits which are formally neutral (like the $\{Cl_2Ru(\mu\text{-}2,3\text{-dpp})_2\}$ component) or doubly charged (like the $\{(\mu\text{-}2,3\text{-dpp})Os(bpy)_2\}^{2+}$ one). The luminescence spectra of **2** (Table 2, Fig. 8), both at room temperature and at 77 K, are very close to those of **6**, so they are attributed to the MLCT levels involving the peripheral components under both conditions.

From the above discussion it can be noted that each subunit of the multinuclear systems maintains its own photophysical properties (mainly, the luminescent energy level) in the multicomponent arrangements, similarly to what happens for the redox properties. However, also as far as the luminescence properties are concerned, slight perturbation of the individual subunits takes place due to the presence of the nearby components. For example, the luminescent MLCT level of **2**, which involves the peripheral $\{(\mu\text{-}2,3\text{-dpp})Os(bpy)_2\}^{2+}$ subunits, is slighly red-shifted for **6** (Table 2), because of the different electron withdrawing ability of the central chromophores of **2** and **6**, as reflected in the reduction potentials of the bridging ligands (see redox properties).

Since the luminescence of all the dendrons (with the exception of **5**) occurs in the near-infrared region, it was impossible to determine the luminescence lifetimes and quantum yields and to obtain reliable excitation spectra because of technical problems. So we could not monitor the occurrence of intercomponent energy transfer for most of the compounds studied here. However, because (i) efficient center-to-periphery energy transfer is demonstrated to occur in **5**,[4a] (ii) the present systems are similar to previously studied analogous systems,[3a] and (iii) alternative decays of the upper-lying MLCT levels are not foreseen (*i.e.* intercomponent electron transfer processes are endoergonic), efficient intercomponent energy transfer is also likely to take place in the dendrons here reported. In particular, it is interesting that the direction of the energy transfer should be controlled by the topology of the species, with center-to-periphery energy transfer taking place in **2**, **5**, and **6** and periphery-to-center processes occurring in the other species.

Conclusion

We have synthesized three new trinuclear dendrons $[Cl_2Os\{(\mu\text{-}2,3\text{-dpp})Ru(bpy)_2\}_2]^{4+}$ **3**, **Cl_2OsRu_2**, $[Cl_2Os\{(\mu\text{-}2,3\text{-dpp})Os(bpy)_2\}_2]^{4+}$ **4**, **Cl_2OsOs_2**, and $[(bpy)Ru\{(\mu\text{-}2,3\text{-dpp})Os(bpy)_2\}_2]^{6+}$ **6**, **$bpyRuOs_2$** and have performed an extensive study of their redox properties, absorption spectra, and luminescence properties. In particular, the trinuclear dendrons **3** and **4** are quite interesting in that they open the way to high generation dendrimers containing osmium centers at intermediate sites, not available up to now. The same redox, spectroscopic and photophysical properties of the already known trinuclear species $[Cl_2Ru\{(\mu\text{-}2,3\text{-dpp})Ru(bpy)_2\}_2]^{4+}$ **1**, **Cl_2RuRu_2**, $[Cl_2Ru\{(\mu\text{-}2,3\text{-dpp})Os(bpy)_2\}_2]^{4+}$ **2**, **Cl_2RuOs_2**, and $[(bpy)Ru\{(\mu\text{-}2,3\text{-dpp})Ru(bpy)_2\}_2]^{6+}$ **5**, **$bpyRuRu_2$** have also been investigated in detail and compared to the properties of the new compounds.

The collected data show that each metal-based subunit maintains to a first approximation its own redox, spectroscopic and photophysical properties in the supramolecular dendron-like structure, and that efficient and directional intercomponent energy transfer processes are accordingly expected to take place within the multicomponent arrays. Furthermore, the redox and luminescence data have made it possible to gain detailed information on the fine interactions between the various subunits in the different compounds. The results are of high interest for designing larger dendritic species with predetermined redox and photophysical properties.

Acknowledgements

Financial support from MURST (Project "Artificial Photosynthesis") and the European Community (TMR Research Project on "Nanometer Size Metal Complexes") is gratefully acknowledged.

References and notes

1 (*a*) J.-P. Sauvage, J.-P. Collin, J.-C. Chambron, S. Guillerez, C. Coudret, V. Balzani, F. Barigelletti, L. De Cola and L. Flamigni, *Chem. Rev.*, 1994, **94**, 993; (*b*) V. Balzani, A. Juris, M. Venturi, S. Campagna and S. Serroni, *Chem. Rev.*, 1996, **96**, 759; (*c*) A. Harriman and R. Ziessel, *Chem. Commun.*, 1996, 1707; (*d*) C. A. Bignozzi, J. R. Schoonover and F. Scandola, *Prog. Inorg. Chem.*, 1997, **44**, 1; (*e*) C. A. Slate, D. R. Striplin, J. A. Moss, P. Chen, B. W. Erickson and T. J. Meyer, *J. Am. Chem. Soc.*, 1998, **120**, 4885; (*f*) E. Zahavy and M. A. Fox, *Chem. Eur. J.*, 1998, **4**, 1647; (*g*) L. De Cola and P. Belser, *Coord. Chem. Rev.*, 1998, **177**, 301; (*h*) Y.-Z. Hu, S. Tsukiji, S. Shinkai, S. Oishi and I. Hamachi, *J. Am. Chem. Soc.*, 2000, **122**, 241; (*i*) F. Barigelletti and L. Flamigni, *Chem. Soc. Rev.*, 2000, **29**, 1.

2 F. Barigelletti, L. Flamigni, J.-P. Collin and J.-P. Sauvage, *Chem. Commun.*, 1997, 333; O. Waldmann, J. Hassmann, P. Müller, G. S. Hanan, D. Volkmer, U. S. Schubert and J.-M. Lehn, *Phys. Rev. Lett.*, 1997, **78**, 3390.

3 (*a*) V. Balzani, A. Juris, M. Venturi, S. Campagna and S. Serroni, *Acc. Chem. Res.*, 1998, **31**, 26; (*b*) V. Balzani and S. Serroni, *Sci. Spectra*, 2000, **22**, 28; (*c*) S. Campagna, S. Serroni, F. Puntoriero and C. Di Pietro, in *Electron Transfer in Chemistry*, ed. V. Balzani, VCH-Wiley, Weinheim, 2001, vol. 5, p. 186.

4 (*a*) G. Denti, S. Campagna, L. Sabatino, S. Serroni, M. Ciano and V. Balzani, *Inorg. Chem.*, 1990, **29**, 4750; (*b*) S. Campagna, G. Denti, S. Serroni, M. Ciano and V. Balzani, *Inorg. Chem.*, 1991, **30**, 3728; (*c*) G. Denti, S. Campagna, S. Serroni, M. Ciano and V. Balzani, *J. Am. Chem. Soc.*, 1992, **114**, 2944; (*d*) S. Campagna, G. Denti, S. Serroni, M. Ciano, A. Juris and V. Balzani, *Inorg. Chem.*, 1992, **31**, 2982; (*e*) S. Serroni, A. Juris, S. Campagna, M. Venturi, G. Denti and V. Balzani, *J. Am. Chem. Soc.*, 1994, **116**, 9086; (*f*) A. Juris, V. Balzani, S. Campagna, G. Denti, S. Serroni, G. Frei and H. U. Güdel, *Inorg. Chem.*, 1994, **33**, 1491; (*g*) V. Balzani, S. Campagna, G. Denti, A. Juris, S. Serroni and M. Venturi, *Sol. Energy Mater. Sol. Cells*, 1995, **38**, 159; (*h*) A. Juris, M. Venturi, L. Pontoni, I. Resino Resino, V. Balzani, S. Serroni, S. Campagna and G. Denti, *Can. J. Chem.*, 1995, **73**, 1875; (*i*) P. Ceroni, F. Paolucci, C. Paradisi, A. Juris, S. Roffia, S. Serroni, S. Campagna and A. J. Bard, *J. Am. Chem. Soc.*, 1998, **120**, 5480; (*j*) M. Marcaccio, F. Paolucci, C. Paradisi, S. Roffia, C. Fontanesi, L. J. Yellowlees, S. Serroni, S. Campagna, G. Denti and V. Balzani, *J. Am. Chem. Soc.*, 1999, **121**, 10081.

5 (*a*) S. Serroni, G. Denti, S. Campagna, A. Juris, M. Ciano and V. Balzani, *Angew. Chem.*, 1992, **104**, 1540; S. Serroni, G. Denti, S. Campagna, A. Juris, M. Ciano and V. Balzani, *Angew. Chem., Int. Ed. Engl.*, 1992, **31**, 1493; (*b*) S. Campagna, G. Denti, S. Serroni, A. Juris, M. Venturi, V. Ricevuto and V. Balzani, *Chem. Eur. J.*, 1995, **1**, 211; (*c*) S. Serroni, A. Juris, M. Venturi, S. Campagna, I. Resino Resino, G. Denti, A. Credi and V. Balzani, *J. Mater. Chem.*, 1997, **7**, 1227.

6 S. Serroni, S. Campagna, G. Denti, A. Juris, M. Venturi and V. Balzani, in *Advances in Dendritic Chemistry*, ed. G. R. Newkome, JAI Press, 1996, vol. 3, p. 61; V. Balzani, A. Juris, M. Pink, M. Venturi, S. Campagna and S. Serroni, in *Conjugated Polymers, Oligomers, and Dendrimers: from Polyacetylene to DNA*, ed. J.-L. Brédas, De Boeck-Université, Bruxelles, 1999, p. 291 and refs. therein.

7 G. R. Newkome, C. N. Moorefield and F. Vögtle, *Dendritic Molecules. Concepts*, *Syntheses*, *Perspectives*, VCH, Weinheim, 1996.

8 S. Serroni, S. Campagna, F. Puntoriero, A. Juris, G. Denti, V. Balzani and M. Venturi, *Inorg. Synth.*, in press.

9 H. A. Goodwin and F. Lions, *J. Am. Chem. Soc.*, 1959, **81**, 6415.

10 (*a*) B. P. Sullivan, D. J. Salmon and T. J. Meyer, *Inorg. Chem.*, 1978, **17**, 3334; (*b*) D. A. Buckingam, F. P. Dwyer, H. A. Goodwin and A. M. Sargeson, *Aust. J. Chem.*, 1964, **55**, 325.

11 G. Denti, S. Serroni, L. Sabatino, M. Ciano, V. Ricevuto and S. Campagna, *Gazz. Chim. Ital.*, 1991, **121**, 37.

12 A. Licciardello, S. Campagna and S. Serroni, work in preparation.

13 J. N. Demas and G. A. Crosby, *J. Phys. Chem.*, 1971, **75**, 991.

14 K. Nakamaru, *Bull. Chem. Soc. Jpn.*, 1982, **55**, 2697.

15 G. A. Crosby, *Acc. Chem. Res.*, 1975, **8**, 231.

16 A. Juris, V. Balzani, F. Barigelletti, S. Campagna, P. Belser and A. von Zelewsky, *Coord. Chem. Rev.*, 1988, **84**, 85.

17 M. K. De Armond and C. M. Carlin, *Coord. Chem. Rev.*, 1981, **36**, 325.

18 A. A. Vlcek, *Coord. Chem. Rev.*, 1982, **43**, 39.

19 M. Venturi, S. Serroni, A. Juris, S. Campagna and V. Balzani, *Top. Curr. Chem.*, 1998, **197**, 193.

20 The situation is reminiscent of the metal–metal interaction in dinuclear ligand-bridged metal complexes, mediated by a superexchange mechanism involving the bridging ligands.[21–23]

21 C. Creutz, *Prog. Inorg. Chem.*, 1983, **30**, 1.

22 G. Giuffrida and S. Campagna, *Coord. Chem. Rev.*, 1994, **135**–**136**, 517 and refs. therein.

23 A. Bencini, I. Ciofini, C. A. Daul and A. Ferretti, *J. Am. Chem. Soc.*, 1999, **121**, 11418.

24 In Fig. 10 remote MLCT transitions, that is transitions between sites which are not directly linked, are disregarded for simplicity. Anyway, such remote transitions are expected to be obscured by the more intense MLCT transitions between directly linked sites and therefore can safely be ignored at a first approximation when discussing the absorption spectra.[4a]

25 P. C. Bradley, N. Kress, B. A. Hornberger, R. F. Dallinger and W. H. Woodruff, *J. Am. Chem. Soc.*, 1989, **111**, 7441; L. F. Cooley, P. Bergquist and D. F. Kelley, *J. Am. Chem. Soc.*, 1990, **112**, 2612; N. H. Damrauer, G. Cerullo, A. Yeh and J. K. McClusker, *Science*, 1997, **275**, 54.

26 P. Belser, A. von Zelewsky, A. Juris, F. Barigelletti and V. Balzani, *Gazz. Chim. Ital.*, 1983, **113**, 731.

27 Ruthenium(II) polypyridine complexes containing chlorides as ligands are hardly luminescent because their MLCT levels are deactivated by metal centered excited states which promote radiationless decay to the ground state.[16,28] However, in the complexes studied here the MLCT states are low enough in energy that contribution of the (higher-lying) MC levels to the photophysical properties can be disregarded.

28 T. J. Meyer, *Pure Appl. Chem.*, 1986, **58**, 1193 and references therein.